ELSEVIER

Clinical Neurophysiology 116 (2005) 532–544

www.elsevier.com/locate/clinph

Long-term prospective on-line real-time seizure prediction

L.D. Iasemidis[a,c,*], D.-S. Shiau[g,l,m], P.M. Pardalos[d,e,f,k], W. Chaovalitwongse[d,l,m], K. Narayanan[a], A. Prasad[a], K. Tsakalis[b,c], P.R. Carney[f,g,h,i,l], J.C. Sackellares[f,g,h,i,j,l,m]

[a]*Department of Bioengineering, Arizona State University, Tempe, AZ, USA*
[b]*Department of Electrical Engineering, Arizona State University, Tempe, AZ, USA*
[c]*Center for Systems Science and Engineering Research, The Harrington Department of Bioengineering, Arizona State University, P.O. Box 879709, Tempe, AZ 85287-9709, USA*
[d]*Department of Industrial and Systems Engineering, University of Florida, Gainesville, FL, USA*
[e]*Department of Computer Science, University of Florida, Gainesville, FL, USA*
[f]*Department of Biomedical Engineering, University of Florida, Gainesville, FL, USA*
[g]*Department of Neuroscience, University of Florida, Gainesville, FL, USA*
[h]*Department of Neurology, University of Florida, Gainesville, FL, USA*
[i]*Department of Pediatrics, University of Florida, Gainesville, FL, USA*
[j]*Department of Psychiatry, University of Florida, Gainesville, FL, USA*
[k]*Center for Applied Optimization, University of Florida, Gainesville, FL, USA*
[l]*McKnight Brain Institute, University of Florida, Gainesville, FL, USA*
[m]*Malcolm Randall V.A. Medical Center, Gainesville, FL, USA*

Accepted 7 October 2004
Available online 6 January 2005

Abstract

Objective: Epilepsy, one of the most common neurological disorders, constitutes a unique opportunity to study the dynamics of spatiotemporal state transitions in real, complex, nonlinear dynamical systems. In this study, we evaluate the performance of a prospective on-line real-time seizure prediction algorithm in two patients from a common database.

Methods: We previously demonstrated that measures of chaos and angular frequency, estimated from electroencephalographic (EEG) signals recorded at critical sites in the cerebral cortex, progressively converge (i.e. become dynamically entrained) as the epileptic brain transits from the asymptomatic interictal state to the ictal state (seizure) (Iasemidis et al., 2001, 2002a, 2003a). This observation suggested the possibility of developing algorithms to predict seizures well ahead of their occurrences. One of the central points in those investigations was the application of optimization theory, specifically quadratic zero-one programming, for the selection of the critical cortical sites. This current study combines that observation with a dynamical entrainment detection method to prospectively predict epileptic seizures. The algorithm was tested in two patients with long-term (107.54 h) and multi-seizure EEG data B and C (Lehnertz and Litt, 2004).

Results: Analysis from the 2 test patients resulted in the prediction of up to 91.3% of the impending 23 seizures, about 89 ± 15 min prior to seizure onset, with an average false warning rate of one every 8.27 h and an allowable prediction horizon of 3 h.

Conclusions: The algorithm provides warning of impending seizures prospectively and in real time, that is, it constitutes an on-line and real-time seizure prediction scheme.

Significance: These results suggest that the proposed seizure prediction algorithm could be used in novel diagnostic and therapeutic applications in epileptic patients.

Keywords: Nonlinear dynamics; EEG; Real-time prospective seizure prediction; Lyapunov exponents; Spatio-temporal transition

1. Introduction

Epilepsy affects approximately 1% of the population. It is characterized by recurrent, paroxysmal (short-term) electrical discharges of the cerebral cortex that result in

* Corresponding author. Tel.: +1 480 965 9134; fax: +1 480 727 7624.
E-mail address: leon.iasemidis@asu.edu (L.D. Iasemidis).

1388-2457/$30.00
doi:10.1016/j.clinph.2004.10.013

intermittent disturbances of brain function (Niedermeyer, 1987; Spencer et al., 1992). Interictally (between seizures), brief paroxysmal spikes (less than 100 milliseconds duration) and spike and slow wave complexes (usually less than 1 s duration), due to synchronous firing of large neuronal populations, appear to occur randomly in the EEG. In seizures of focal onset (focal seizures, partial seizures), the anatomical distribution of the interictal spikes varies, but spikes tend to occur most commonly in the epileptogenic zone and its connections. During the seizure, organized, quasi-synchronized, quasi-rhythmic electrical discharges develop in the epileptogenic zone and spread, within seconds, over widespread areas of cerebral cortex. Seizure discharges typically last seconds to minutes and are followed by postictal slowing and disorganization of background EEG rhythms. Seizures severely disrupt normal brain functions. Thus, they can incapacitate the patient during and for some time after the seizure.

In partial epilepsy, there are structural changes in neuronal circuitry within localized regions of the cerebral neocortex or hippocampus. The seizure onset zone typically centers around these areas of anatomical abnormalities. The hippocampus is the most common location of an epileptogenic focus. Structural abnormalities in the epileptogenic hippocampus include neuronal loss, altered neurotransmitter receptor density, dendritic simplification, and axonal sprouting of dentate granule cells (Babb and Brown, 1987; Burdette et al., 1995; De Lanerrole et al., 1989; McDonald et al., 1991; Pennell et al., 1999; Savic et al., 1988). Metabolic abnormalities in epileptogenic regions during the interictal (between seizures) state have been observed. Localized zones of hypometabolism are detectable interictally with positron emission tomographical (PET) scans (Abou-Khalil et al., 1987). Although macroscopic and microscopic features of the epileptogenic zone have been described, the mechanism by which these fixed in time structural abnormalities in local circuitry produce intermittent disturbances of brain function is not understood yet.

Through mathematical analysis of the spatiotemporal dynamics EEG recordings in patients with medically intractable (antiepileptic drug resistant) temporal lobe epilepsy, Iasemidis and Sackellares discovered a preictal transition that precedes seizures for periods on the order of minutes to hours (Iasemidis and Sackellares, 1991, 1996; Iasemidis et al., 1996, 1997, 2000a; Sackellares et al., 1999, 2000). This preictal dynamical transition is characterized by a progressive convergence (dynamical entrainment) of dynamical measures (e.g. short-term maximum Lyapunov exponents—STLmax) at specific anatomical areas in the neocortex and hippocampus. STLmax, measured in bits/s, corresponds to the maximum rate of generation or destruction of information as it is detected in the EEG signal (Iasemidis et al., 1990, 2000b; Kostelich, 1992; Vastano and Kostelich, 1986; Wolf et al., 1985). Although the existence of the preictal transition period has recently been confirmed and further defined by other investigators (Elger and Lehnertz, 1998; Le Van Quyen et al., 1999, 2001; Lehnertz and Elger, 1998; Martinerie et al., 1998), the characterization of this spatiotemporal transition is still far from complete. Therefore, the development of a model for the mechanism of generation of epileptic seizures remains a difficult task. For example, even in the same patient, different sets of cortical sites may exhibit preictal entrainment from one seizure to the next. In addition, resetting of the dynamical entrainment of the normal sites with the epileptogenic focus (critical brain sites) occurs after each seizure (Iasemidis et al., 2003b, 2004a; Sackellares et al., 1997, 2002; Shiau et al., 2000). Therefore, we postulate that complete or partial postictal resetting of preictal entrainment of the epileptic brain affects the route to the subsequent seizure, contributing to the apparently non-stationary nature of the dynamical entrainment process. Even though a complete modeling of the process remains elusive, the dynamical measures we have used have resulted in the development of effective seizure prediction schemes.

The ability to predict an impending seizure well ahead of its clinical or electroencephalographic onset provides an opportunity for new diagnostic and therapeutic applications that could revolutionize the medical and surgical management of epilepsy (Witte et al., 2003). Control of seizures through electrical, magnetic stimulation of the brain or its connections, or pulsed pharmacological intervention is a rapidly developing field (for a recent review see Iasemidis, 2003). Stimulation via implanted neurostimulators in the brain is currently considered a promising new form of treatment (functional neurosurgery) for various brain disorders (e.g. epilepsy, Parkinsons' and other neurodegenerative diseases). A reliable prediction of seizures in epilepsy, as well as of critical transitions in other neurological disorders, may provide the answer to the question of when and where to stimulate in the brain to accomplish the disruption of the route toward these undesirable transitions (closed loop control schemes; Iasemidis et al., 2003c). In this manuscript, we present the results of the application of our prediction algorithm to long-term EEGs with multiple seizures from two patients (B and C) with temporal lobe seizures stored in a common database established from contributions of several epilepsy centers (Lehnertz and Litt, 2004).

The organization of this paper is as follows. Definition and the method of estimation of STLmax measures from the EEG are described in Section 2. The selection of specific cortical areas, using optimization theory, to maximize the detection of the preictal transition is addressed in Section 3. In Section 4, the method of predicting impending epileptic seizures is presented. Sensitivity and specificity results of the prediction scheme are presented in Section 5. These results are discussed in the final Section 6.

2. Methods

2.1. STLmax as a nonlinear dynamical measure of the EEG

Since the time of its discovery by Richard Caton and its systematic investigation by Hans Berger, the EEG has been the most utilized signal for clinical assessment of brain function. Unfortunately, traditional signal processing theory, based on very simple assumptions about the system that produces the signal (e.g. linearity assumption) has met the challenge of quantification of EEG with varying degrees of success. This limitation is imposed by the fact that the EEG is generated by a nonlinear system, the brain. EEG characteristics such as alpha activity and seizures, normal characteristics such as bursting behavior during light sleep, amplitude dependent frequency behavior (the smaller the amplitude the higher the EEG frequency) and the existence of frequency harmonics (e.g. under photic driving conditions) are typical features of the EEG signal. These properties are characteristics of typical nonlinear systems. The EEG is the output of a non-stationary multidimensional system. Thus, it has statistical properties that depend on both time and space (anatomical location within the brain). Nonlinear components of the brain (neurons) are densely interconnected and the EEG recorded from one site is inherently related to the activity at other sites. These components interact functionally at various points in time. As a result, the EEG is a multivariable, nonlinear, non-stationary time series (Jansen, 1991).

An established technique for visualizing the dynamical behavior of a multivariable system is to generate a state space portrait of the system. A state space portrait is created by treating each time-dependent variable of the system as a component of a vector in a multidimensional space, the state space of the system. Each vector in the state space represents an instantaneous state of the system. These time-dependent vectors are plotted sequentially in the state space to represent the evolution of the state of the system over time. In principle, analysis of a single observable (e.g. EEG recorded from one electrode) can provide information about other system variables that are related to that observable (e.g. activities at other electrode sites). Thus, it is possible to understand important features of a dynamical system through analysis of a single observable over time. Through the method of delays described by Packard et al. (1980) and Takens (1981), sampling of a single observable over time can approximate the position (state) of the system in a space spanned by the system variables related to this observable. Sampling with the method of delays can be used to reconstruct a multidimensional state space from a single-channel EEG signal (Babloyantz and Destexhe, 1986; Casdagli et al., 1996; Iasemidis et al., 1993, 1994). In such an embedding, each state is represented in the state space by a vector $X(t)$ whose components are the delayed versions of the original single-channel EEG time series $u(t)$, that is, $X(t)=[u(t),u(t-\tau),\ldots,u(t-(p-1)\tau)]$, where $X(t)$ is a vector in the state space at time t, τ is the time delay between successive components of $X(t)$, and p is the embedding dimension of the reconstructed state space.

In a chaotic system, orbits originating from similar initial conditions (nearby points in the state space) diverge exponentially (expansion process). The rate of divergence is an important aspect of the system dynamics and is reflected in the value of Lyapunov exponents. The measures that quantify the chaoticity of an attractor are Kolmogorov entropy and the Lyapunov exponents, typically measured in bits/s (Abarbanel, 1996; Oseledec, 1968; Pesin, 1977; Walters, 1982). For an attractor to be chaotic, the Kolmogorov entropy, or at least the maximum Lyapunov exponent (Lmax), must be positive. Methods for calculating these dynamical measures from experimental data have been published (Iasemidis et al., 1990, 2000b; Vastano and Kostelich, 1986; Wolf et al., 1985). Lmax measures the local stability of the state of the system on average. When the structure of the system changes over time, for example as interactions of multiple brain sites change signs and intensity within msecs, only approximations of Lmax of states of the system within a short time interval can be defined. The short-term maximum Lyapunov exponent (STLmax) has been proposed as a measure of chaos in such situations (Iasemidis and Sackellares, 1991, 1996; Iasemidis et al., 2000b). In addition, it is shown that the spatiotemporal convergence of STLmax leads to prediction of epileptic seizures, despite recent reports in the literature on the inability of *Lmax* to predict seizures (Lai et al., 2003, 2004). Those authors failed in their attempts to properly estimate Lmax (using an inappropriate algorithm suitable only for stationary systems, as well as the wrong embedding) and ignored the spatial dynamics of the epileptic brain (Iasemidis et al., 2004b).

EEG recordings from multiple sites in the cerebral neocortex and hippocampus were performed for clinical diagnostic purposes in two patients with refractory epilepsy (see Table 1). Electrode montages for these recordings are provided in the accompanying paper by Lehnertz and Litt (2004). The EEG onset of a typical epileptic seizure of a focal origin from patient C is illustrated in Fig. 1.

In Fig. 2, the STLmax profile (i.e. STLmax values over time long prior and after a seizure) at one electrode site is illustrated. The analyzed EEG includes the seizure depicted in Fig. 1. The seizure lasted about 2 min and occurred about 128 min into the displayed record (seizure onset at the first vertical line in the figure). The state space was reconstructed

Table 1
Characteristics of analyzed EEG datasets

Patient	Number of analyzed seizures	Total length of data (h)	Average inter-seizure time (h)	Inter-seizure time range (h)
C	15	54.12	3.87 ± 0.95	1.63–8.43
B	10	53.42	5.93 ± 1.59	1.60–13.22
All patients	25	107.54	4.67 ± 0.85	1.60–13.22

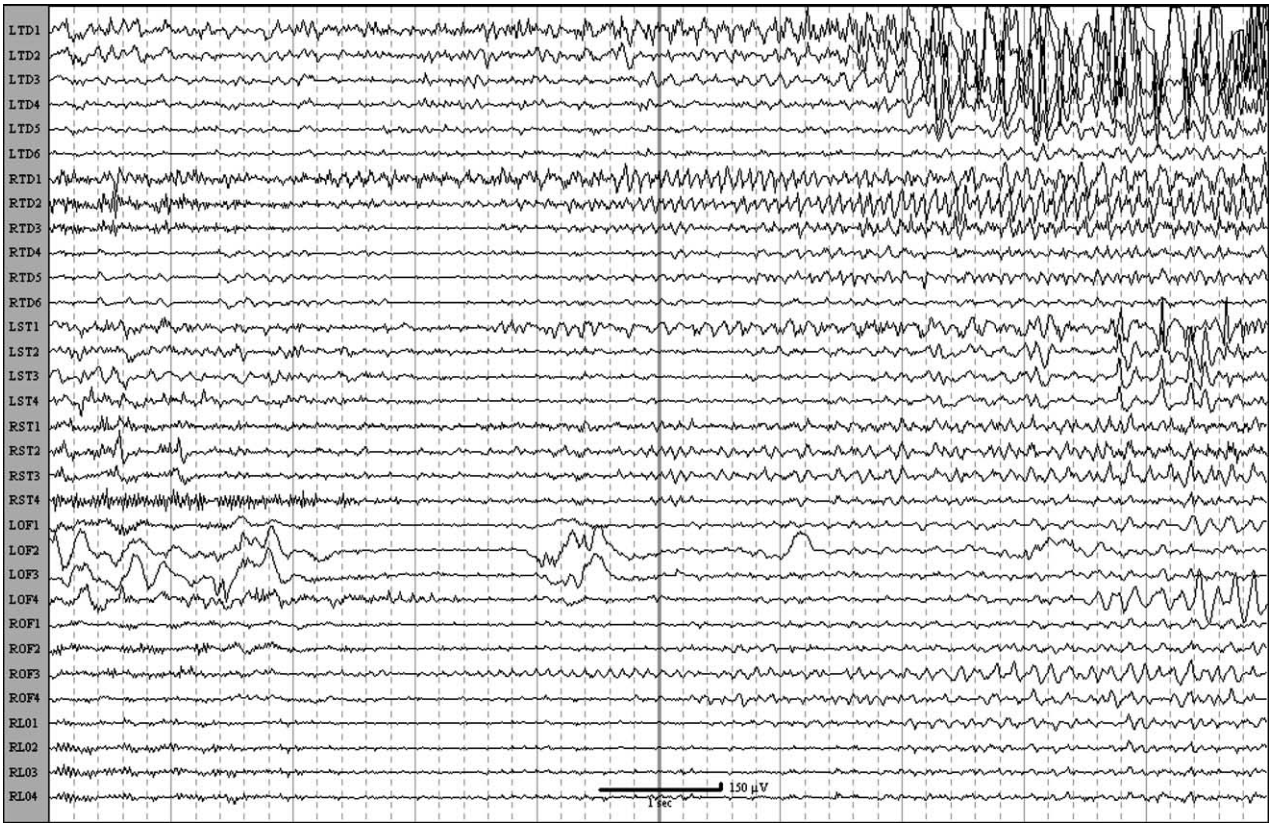

Fig. 1. Ten-second EEG recording of the onset of a typical epileptic seizure from patient C (for electrode montage see Lehnertz and Litt, 2004)). Solid vertical gray lines occur at 1 s intervals. The seizure (ictus) begins as an organized quasi-rhythmic discharge involving the right amygdale and hippocampus (RTD 1–3) and spread to the remaining right temporal depth electrodes, then to the right subtemporal (RST) and orbitofrontal (ROF) regions, and finally the left temporal structures (LTD and LST). As the seizure evolves, the ictal discharges spread to all electrode sites in both cerebral hemispheres.

from sequential, non-overlapping EEG data segments of 2048 points (sampling frequency 200 Hz, hence each segment of 10.24 s in duration) with $p=7$ and $\tau=4$. The preictal, ictal and postictal states correspond to medium, low and higher values of STLmax, respectively. The lowest STLmax values were observed during the ictal period, and lower STLmax values were observed during the preictal period than during the postictal period. However, these observations taken at one electrode site can hardly denote a long-term warning of an impending seizure.

2.2. Spatial dynamical entrainment of STLmax before an epileptic seizure

STLmax profiles per available electrode site were estimated according to the procedure described. The STLmax profiles shown in Fig. 3 denote a convergence of the STLmax values before seizures. We have called this convergence 'dynamical entrainment' and we have quantified it by a T-statistic.

The T-index, the test statistic from the well-known paired-t test for comparisons of means of paired-dependent observations, was employed as a measure of statistical distance between pairs of STLmax profiles over a time window. The $T_{i,j}$ index at time t between the STLmax profiles of electrode sites i and j is then defined as

$$T_{ij}(t) = \frac{|\bar{D}_{ij}^t|}{\hat{\sigma}_{ij}^t/\sqrt{N}}$$

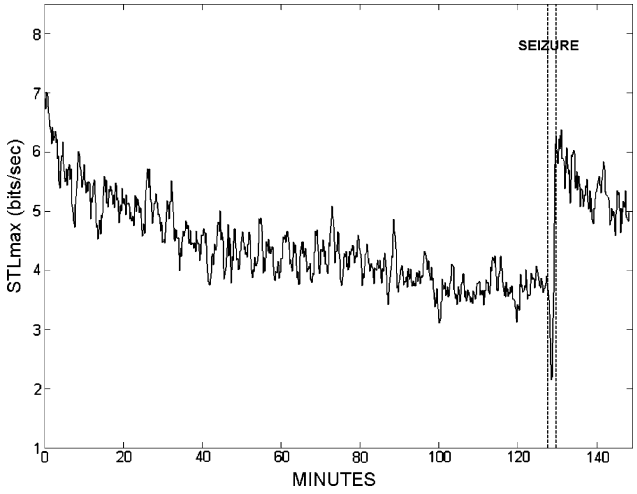

Fig. 2. STLmax profile, after seizure no. 12 and before, during and after epileptic seizure no. 13 recorded from patient C. It is estimated by the analysis of the EEG recorded from a site in the right epileptogenic hippocampus (RTD1). The seizure onset was at the vertical line and the ictal period lasted about 2 min.

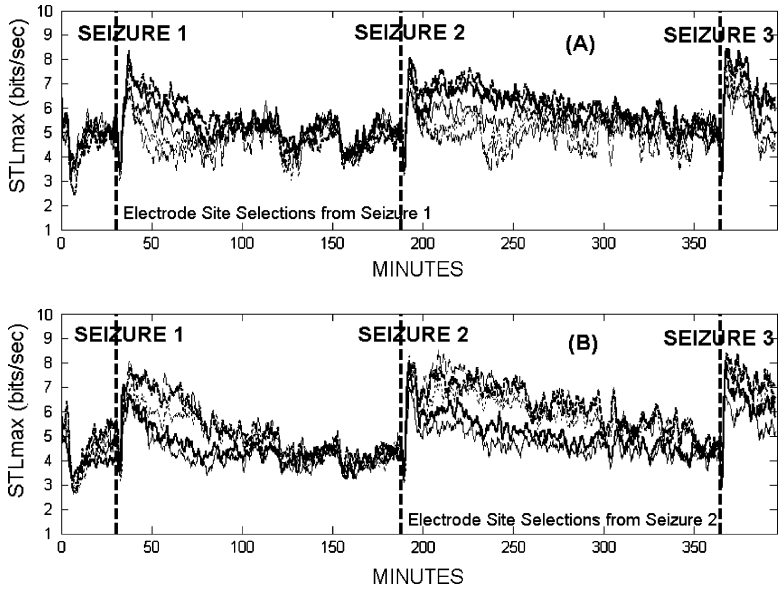

Fig. 3. STLmax profiles at the optimal groups of sites, starting 30 min before seizure no. 1 through 30 min after seizure no. 3, selected based on dynamical entrainment/disentrainment (a) at seizure no. 1, and (b) at seizure no. 2. For both groups of sites, the STLmax profiles gradually converge before seizures no. 2 and no. 3 (Patient C).

where $|\bar{D}_{ij}^t|$ denotes the absolute value of the average of all pairwise differences $D_{ij}^t = \{\text{STLmax}_i^t - \text{STLmax}_j^t | t \in w(t)\}$ within a moving window $w(t)$ defined as

$$w(t) = \left[\frac{t}{10.24s} - N + 1, \frac{t}{10.24s}\right]$$

where N is the length (no. of STLmax points) of the moving window and $\hat{\sigma}_{ij}^t$ is the sample standard deviation of D_{ij} within $w(t)$. Asymptotically, $T_{i,j}(t)$ index follows a t-distribution with $N-1$ degrees of freedom (Iasemidis et al., 2004a).

In the estimation of the $T_{i,j}(t)$ indices from our data, we used $N=60$ (i.e. averages of 60 differences of STLmax values per moving window). Since each value in the STLmax profiles is derived from a 10.24 s EEG data segment, the length of the window used corresponds to approximately 10 min in real time units. A critical value $T_{\alpha/2}$ from the t-distribution with $N-1$ ($=59$) degrees of freedom at significance level α ($=0.01$), is used to test the null hypothesis H_0: "brain sites i and j acquire identical STLmax values within time window $w_t(\lambda)$". For the T-index to reject H_0, $T_{i,j}(t)$ should be greater than $T_2=2.662$ ($=T_{0.005,59}$).

An example of average T-index profiles across electrodes (the STLmax profiles of the selected groups of electrodes are shown in Fig. 3) is shown in Fig. 4. Each of these profiles is estimated according to the previously described procedure for all possible pairs of the five electrode sites, selected from seizure no. 1 in Fig. 4A and from seizure no. 2 in Fig. 4B, and then taking the average of the estimated pair T-indices over time. In both figures, three groups of electrodes were selected based on the dynamical entrainment/disentrainment at seizure no. 1 (Fig. 4A) or seizure no. 2 (Fig. 4B). Two critical T-index thresholds for disentrainment $T_1=5.000$ ($\alpha<0.00001$) and entrainment $T_2=2.662$ ($\alpha=0.01$) are also shown as horizontal lines. From inspection of this figure, it is clear that the considered electrode sites are dynamically entrained at the 0.01 significance level ($T<T_2$) from about 10 to 90 min prior to the seizures. We have developed an optimization procedure that automatically selects the most critical cortical sites participating in the preictal transition from all possible combinations of cortical sites.

While the preictal state is usually associated with convergence in dynamical measures estimated from EEG signal recorded from multiple electrode sites, the specific sites involved vary from seizure to seizure, even in the same patient. However, electrode sites that participated in the preictal convergence preceding a given seizure are most likely to participate in the preictal transition preceding the next seizure. Thus, those electrode sites that converged prior to the most recent seizure are good candidate sites to monitor in an attempt to predict the next seizure. An on-line, real-time seizure prediction scheme requires rapid identification of candidate electrode pairs, a task that can be computationally intense. A practical seizure prediction device must be able to accomplish this step within seconds to a few minutes. Motivated by the application of the Ising model to phase transitions (Pardalos and Rodgers, 1989, 1990), we have applied quadratic bivalent (zero–one) programming for the selection of the most critical cortical sites at periods prior to epileptic seizures (preictal periods) (Iasemidis et al., 2000a, 2001, 2002a, 2003a). The objective function to be minimized was the distance of measures of STLmax (Iasemidis et al., 2000a, 2001) or average angular frequency $\bar{\Omega}$ (Iasemidis et al., 2002a, 2003a) between cortical recording sites during the preictal period. The sites

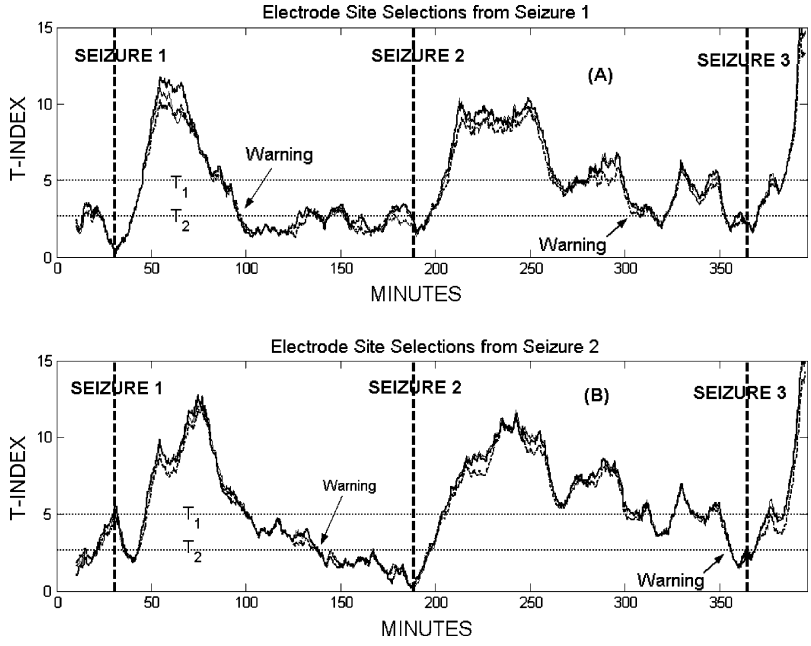

Fig. 4. The average T-index profiles of the most optimal group of electrode sites (depicted in Fig. 3) and of the next two suboptimal ones. Three groups of electrodes were selected (STLmax profiles of the groups in solid bold line were shown in Fig. 3) based on the dynamical entrainment/disentrainment (a) at seizure no. 1 and (b) at seizure no. 2. The two critical values $T_1=5.000$ ($\alpha<0.00001$) and $T_2=2.662$ ($\alpha=0.01$) are also shown as horizontal lines. The selected groups of electrode sites are dynamically entrained at the 0.01 significance level ($T<T_2$) about 10 to 90 min prior to the seizures. All groups of electrode sites are disentrained after the end of the seizures (Patient C).

selected by the optimization method have provided two important insights. First, the most optimal sites participating in the preictal transition could be identified in this way. Second, convergence of dynamical measures of the selected sites over time (dynamical entrainment) could be detected well before the onset of an impending epileptic seizure.

More specifically, we considered the integer 0–1 problem $P1$:

$$P1: \text{minimize}(x^T \boldsymbol{T} x)$$
$$\text{subject to} \sum_{i=1}^{n} x_i = k \qquad (1)$$
$$x \in \{0,1\}^n$$

where n is the total number of electrode sites and k the number of sites to be selected. The elements of the symmetric matrix $\boldsymbol{T}_{n\times n}$ are the all possible T-index values T_{ij}s ($T_{ij}=T_{ji}$, $T_{ii}=0$) within 10 min windows $w(t)$ located 10 min before the onset of a seizure. The algorithm gives the optimal tuple of k sites, that is, the sites for which the average T-index over all possible pairs within the tuple attains a global minimum (Iasemidis et al., 2001).

Previous studies by our group have shown that measures of the spatiotemporal dynamical properties STLmax profiles demonstrate resetting of the brain after seizures' onset (Iasemidis et al., 2003b, 2004a; Sackellares et al., 1997, 2002; Shiau et al., 2000), that is, divergence of STLmax profiles (dynamically disentrained) after seizures. Therefore, to ensure that the optimal tuple of critical sites shows this disentrainment after the seizure, we reformulated the optimization scheme by adding one more quadratic constraint. More specifically, this optimization problem becomes quadratic integer 0–1 problem with quadratic knapsack constraint $P3$:

$$P3: \text{minimize}(x^T \boldsymbol{T} x)$$
$$\text{subject to} \sum_{i=1}^{n} x_i = k \qquad (2)$$

$$x^T \boldsymbol{Q} x > T_1 \binom{k}{2} \qquad (3)$$
$$x \in \{0,1\}^n$$

The elements of the matrix $\boldsymbol{Q}$ are the all possible T-index values within 10 min windows after the end of a seizure. T_1 is the critical value of T-index, as previously defined, to reject H_0: "two brain sites acquire identical STLmax values within time window $w(t)$".

Figs. 5 and 6 illustrate the results of the application of the above procedure to the detection of the preictal transition preceding seizure no. SC3 in patient B. The STLmax profiles from 3 electrode sites (k=3), selected with the optimization program applied during the 10 min interval immediately preceding the onset of seizure no. SC2 are shown in Fig. 5. The average T-index over all possible T_{ij} indices among the optimal 3 sites is plotted over time in Fig. 6. Several points are noteworthy. First, the use of optimal sites for the estimation of STLmax and average T-index profiles helps to detect the preictal transition

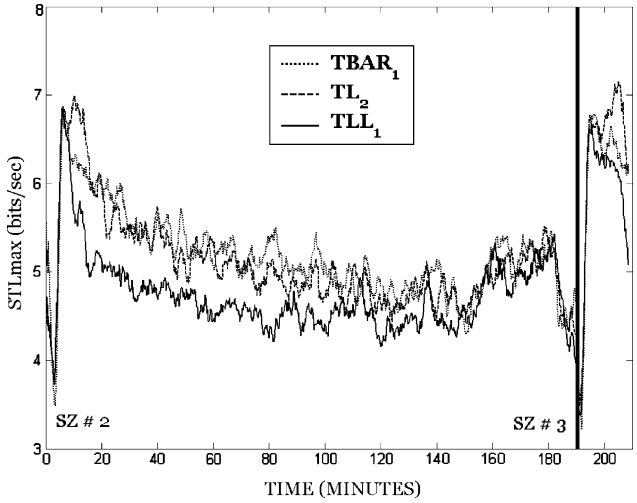

Fig. 5. STLmax profiles, after seizure no. 2 and before, during and after epileptic seizure no. 3 recorded from patient B. They are estimated by analysis of the EEG recorded from a site in the left epileptogenic hippocampus (TL), one site in the ipsilateral hemisphere (TLL1—left medial temporal gyrus), and one site in the contralateral hemisphere (TBAR1—right temporal cortex). The seizure onset was at the vertical line (Patient B).

(see next section) about 90 min prior to this seizure (i.e. at approximately 110 min into the recording shown in Fig. 6). The warning flag is raised when the average T-index value crosses threshold T_2 (i.e. sites become entrained) under the condition that it crossed T_1 before (i.e. sites were well disentrained before they started to become entrained and the algorithm to start monitoring them).

2.3. Prediction of epileptic seizures

Results from the application of the previously described analytic scheme to the EEG data for the prediction of 23 out of the 25 recorded seizures (first seizure per patient is not to be predicted but it is instead used to initialize the algorithm with respect to selection of critical sites) are to be presented in this section.

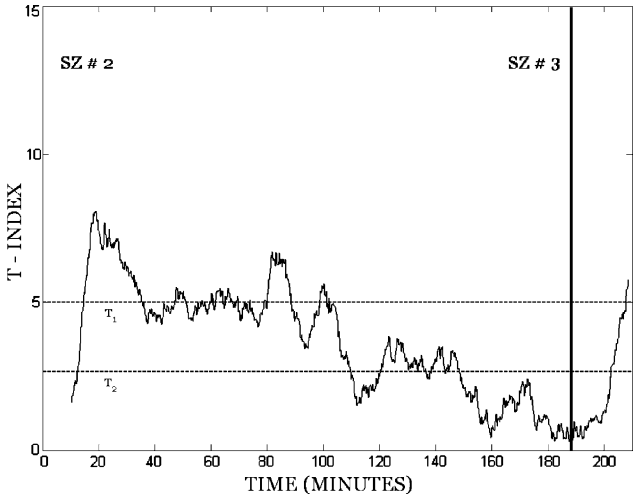

Fig. 6. The average T-index profile of the 3 optimal electrode sites whose STLmax profiles are depicted in Fig. 4. The 3 sites become dynamically entrained approximately 80 min prior to the onset of seizure 15. They are disentrained after the end of the seizure (Patient B).

We showed previously that detection of the preictal transition is possible by a dynamical analysis of the EEG retrospectively, that is after the occurrence of a seizure (Iasemidis et al., 2000a, 2001). However, the prospective detection of the preictal transition that is well before the occurrence of an epileptic seizure constitutes seizure prediction. It is now clear that the prospective detection of the preictal transition depends heavily on appropriate selection of the cortical sites that are likely to participate in the next preictal transition. Therefore, prospective selection of participating sites and monitoring of their average T-index value over time are critical components in a prediction scheme. Also, a prediction scheme should be evaluated in terms of its sensitivity (true positives rate) and false positive rate (per hour) to the occurrences of epileptic seizures.

The seizure prediction algorithm (SPA) we have devised consists of the following steps:

2.3.1. On-line, continuous calculations of STLmax profiles

Segmentation of continuous EEG into consecutive non-overlapping segments of 10.24 s in duration per electrode site constitutes the first step. The construction of the state space with $p=7$ and $\tau=4$ per EEG segment is the second step (Iasemidis et al., 1990, 2000b). The estimation of STLmax per segment is the next step. The STLmax algorithm is then applied sequentially to non-overlapping segments from each EEG channel, creating a new multi-channel time series STLmax(t) that is utilized for subsequent analysis.

2.3.2. Estimation of the T-index profiles

Taking 60 consecutive STLmax values per channel (i.e. real time span of each window of STLmax values is about 10 min), and applying the procedure of the previous section, the T-index matrix is estimated (its components are the T_{ij}, with i and $j=1,\ldots,n$, where n is the total number of EEG channels present). The estimation of the T-index matrix is performed in a 10-min interval prior to each seizure, and it is subsequently used for the prediction of the next seizure.

2.3.3. Optimization (selection of critical electrode sites)—estimation of the average T-index profiles

After the occurrence of the first seizure, k critical electrode sites are identified. The average T-index is then estimated as the average value of the T_{ij}s of all pairs (i, j) of the identified critical sites, and it is subsequently monitored forward in time. Selection of critical electrode sites is accomplished in two steps. First, applying the optimization procedure described in the previous section, the k electrode sites that are most entrained (their average T-index is a global minimum) during the 10-min epoch prior to a seizure,

and are also disentrained after that seizure, are identified. An efficient quadratic global optimization programming was employed toward this direction (Pardalos and Rodgers, 1989, 1990). These selection criteria were chosen to ensure selection of groups of sites that are most entrained prior to the first seizure and become disentrained after that seizure. These criteria are based on the hypothesis that seizures occur to reset the preictal entrainment of critical sites in the cerebral cortex (Iasemidis et al., 2003b, 2004a; Sackellares et al., 1997, 2002; Shiau et al., 2000). Second, in addition to the most critical group ($g=1$) of k sites thus defined, the next critical groups of k sites, that is those sites that have the next lowest average T-indices preictally and are disentrained postictally, were identified. It is clear that if we have n recording sites, there are $\binom{n}{k}$ number of possible groups of k sites. Through an exhaustive search over all possible groups of k sites, the groups were ordered according to their average T-indices, and the groups with the smallest average T-indices were identified. In this way, for each patient, after the first seizure, the optimal g critical groups of k sites were identified. Therefore, only groups with average T-index-preictal less than 2.662 ($t_{\alpha/2,59}=2.662$ for $\alpha=0.01$) in the window of 10 min before the first seizure's onset, conditioned on average T-index-postictal larger than 2.662 in the 10 min window after that seizure's end (i.e. disentrained sites) are selected. However, with large values of k (e.g. $k>6$), it is almost impossible to perform the exhaustive search. The critical electrode sites are updated automatically after each subsequent electrographic seizure, using the optimization technique described for the first seizure.

2.3.4. Warning of an impending seizure

An impending seizure is predicted when a dynamic transition is detected. The method for detecting the transition is described below. After g groups of k sites are selected from the preictal and postictal state of the first seizure, the average T-index of each of the g groups is estimated forward in time every 10.24 s. The average T-index of any of the g groups of sites will be postictally above 2.662 by construction (since sites within a group are disentrained postictally). If and when these sites become entrained in the future, a dynamical transition that may be indicative of an upcoming seizure is announced. In order to make such a conjecture more conservative, we defined a preictal dynamical transition as follows:

A dynamical transition toward a seizure is announced at time t^* when any of the T-indices of the monitored g groups of sites transits over time from a value above 5.000 (threshold T_1) at time $t'<t^*$, to a value below 2.662 (threshold T_2) at time t^*.

Therefore, the T-index curves of each group are continuously compared to the two preset threshold values. The threshold $T_1=5.000$ ($\alpha<0.00001$) is set as the initial condition to begin checking for a transition. When $T>T_1$, the sites in the group are highly disentrained. We expect that it is when these highly disentrained sites become entrained, that an impending seizure is imminent. Once the average T-index curve of one of the selected g groups is above T_1, we follow it forward in time. A dynamical transition is detected if the curve is gradually decreasing and crosses the second threshold value, $T_2=2.662$ ($\alpha=0.01$). A warning of an impending seizure is then issued. A dynamical transition is announced if any of the initially selected g groups of sites provides a warning.

2.3.5. Evaluation of the seizure prediction scheme

To evaluate the seizure prediction scheme, a prediction was considered to be true if a seizure occurred within 2 or 3 h after a warning (dynamical transition) was observed, and false otherwise. That is, a *prediction horizon* (2 or 3-h period) was chosen for the evaluation of the prediction results of the algorithm. This time interval was chosen because previous studies indicated that the preictal transition (as defined by STLmax) might be detectable up to several hours before some seizures. In a practical clinical application, the prediction horizon could be set to give the most appropriate sensitivity and false positive rate for this application. Long-prediction horizons obviously improve the sensitivity of the algorithm but also increase the uncertainty about the exact detection time of the next seizure. If no seizure occurred within the specified horizon, the warning was considered to be false. If a seizure occurred without a warning during the preceding 2 or 3 h, the algorithm was considered to have failed in the prediction of that seizure. Therefore, the sensitivity (S) of the prediction scheme is defined as the total number of seizures accurately predicted divided by the total number of seizures that occurred. The *false* prediction rate (FPR) was defined as the average number of false predictions (warnings) per hour. The average warning time (AWT) of a seizure was defined as the average of the intervals between all true warning times and the subsequent actual seizure onset. Results on S, FPR and AWT are given in the next section.

3. Results

We tested the prediction scheme within a range of parameter settings (k, g), that is, with g from 1 to 5 and k from 3 to 6, to identify the setting that provided minimum overall sensitivity larger than 75% with the lowest rate of false positive predictions. The sensitivity (S), false prediction rate (FPR) and average warning time (AWT) results for each of these parameters are given in Tables 2 and 3 for patient C with prediction horizon of 3 and 2 h, and Tables 4 and 5 for patient B with prediction horizon of 3 and 2 h, respectively. The optimal results are summarized in Table 6. The percentage of seizures that were correctly predicted ranged from 85.71% (12/14—patient C) to 100% (9/9—patient B), with an average across patients of 91.30%

Table 2
Selection of k_{opt} and g_{opt}. Performance characteristics of SPA, with a 3-h prediction horizon, for different parameters (g, k) (seizure dataset from patient C)

No. of critical sites (k)	No. of critical groups (g)	Sensitivity (%)	FPR	Average warning time	
3	1	64.29	0.074	76.06	14.722
3	2	85.71	0.111	75.876	13.975
3	3	85.71	0.148	66.688	13.402
3	4	78.57	0.166	61.331	12.396
3	5	78.57	0.166	62.169	12.487
4	1	50.00	0.037	81.14	15.778
4	2	50.00	0.037	95.915	19.391
4	3	64.29	0.074	84.385	16.985
4	4	64.29	0.092	84.84	17.038
4	5	78.57	0.111	78.414	16.598
5	1	57.14	0.018	62.101	12.314
5	2	64.29	0.055	55.429	12.703
5	3	78.57	0.055	74.954	15.422
5	4	78.57	0.074	73.992	14.024
5	5	78.57	0.074	76.133	15.142
6	1	57.14	0.055	61.227	12.521
6	2	64.29	0.055	80.062	12.539
6	3	64.29	0.055	83.115	14.383
6	4	71.43	0.055	96.666	15.589
6	5	71.43	0.074	96.887	15.586

Table 4
Selection of k_{opt} and g_{opt}. Performance characteristics of SPA, with a 3-h prediction horizon, for different parameters (g, k) (seizure dataset from patient B)

No. of critical sites (k)	No. of critical groups (g)	Sensitivity (%)	FPR	Average warning time	
3	1	55.56	0.056	83.456	20.125
3	2	77.78	0.112	107.252	20.446
3	3	100.00	0.131	105.017	15.176
3	4	100.00	0.131	106.06	15.584
3	5	100.00	0.131	106.458	15.753
4	1	22.22	0.056	72.448	26.248
4	2	66.67	0.075	116.594	18.144
4	3	66.67	0.094	96.796	20.364
4	4	77.78	0.094	93.477	17.783
4	5	66.67	0.112	92.843	20.041
5	1	22.22	0.056	147.115	7.361
5	2	33.33	0.056	155.364	8.334
5	3	44.44	0.056	123.819	31.903
5	4	44.44	0.056	128.384	28.061
5	5	33.33	0.075	122.14	27.521
6	1	22.22	0	72.789	34.213
6	2	66.67	0.019	84.48	27.988
6	3	66.67	0.037	84.48	27.988
6	4	66.67	0.037	94.236	25.507
6	5	66.67	0.056	111.303	23.729

sensitivity using the 3-h prediction horizon. Using the same prediction horizon (3-h), the corresponding values for the FPR were 0.111 to 0.131 per hour, with an average across patients of 0.121 per hour (or one false warning every 8.27 h), and an average warning time of 89 ± 15 min. We note that FPR does not depend on the length of the interseizure intervals. This can be shown if we compare the FPRs observed in both patients. Using the optimal values for g and k at the same prediction horizon (see Table 6), the FPRs of these patients are comparable, even though the mean values of the interseizure intervals of the data analyzed are considerably different (see Table 1).

Table 3
Selection of k_{opt} and g_{opt}. Performance characteristics of SPA, with a 2-h prediction horizon, for different parameters (g, k) (seizure dataset from patient C)

No. of critical sites (k)	No. of critical groups (g)	Sensitivity (%)	FPR	Average warning time	
3	1	50.00	0.111	59.514	13.23
3	2	78.57	0.185	53.558	9.822
3	3	78.57	0.222	61.874	10.658
3	4	85.71	0.222	61.497	9.923
3	5	85.71	0.222	62.293	10.022
4	1	35.71	0.074	59.563	12.167
4	2	35.71	0.092	46.933	15.957
4	3	50.00	0.129	45.909	11.824
4	4	57.14	0.148	47.659	10.613
4	5	71.43	0.166	53.879	11.734
5	1	57.14	0.018	62.101	12.314
5	2	64.29	0.055	55.429	12.703
5	3	57.14	0.111	50.645	13.129
5	4	57.14	0.129	55.275	13.761
5	5	57.14	0.129	55.339	13.734
6	1	57.14	0.055	61.227	12.521
6	2	57.14	0.074	71.232	10.549
6	3	57.14	0.074	71.445	10.423
6	4	50.00	0.111	69.608	11.778
6	5	50.00	0.129	69.925	11.872

Table 5
Selection of k_{opt} and g_{opt}. Performance characteristics of SPA, with a 2-h prediction horizon, for different parameters (g, k) (seizure dataset from patient B)

No. of critical sites (k)	No. of critical groups (g)	Sensitivity (%)	FPR	Average warning time	
3	1	33.33	0.094	48.299	8.561
3	2	44.44	0.206	44.16	8.348
3	3	66.67	0.243	61.127	8.799
3	4	77.78	0.243	56.003	8.91
3	5	88.89	0.243	54.443	7.931
4	1	22.22	0.056	72.448	26.248
4	2	33.33	0.169	49.778	7.429
4	3	44.44	0.169	53.547	11.916
4	4	55.56	0.169	57.549	10.386
4	5	55.56	0.169	62.293	12.668
5	1	0.00	0.094	–	–
5	2	0.00	0.112	–	–
5	3	11.11	0.131	16.043	0
5	4	22.22	0.131	34.133	0.121
5	5	33.33	0.131	52.907	8.022
6	1	11.11	0.019	24.405	0
6	2	55.56	0.056	41.847	18.22
6	3	55.56	0.075	41.847	18.22
6	4	55.56	0.075	53.555	18.328
6	5	44.44	0.112	57.899	22.39

Table 6
Performance characteristics of SPA in two patients B and C with optimal values for the parameters (g, k) per prediction horizon of 2 or 3 h

Training parameters						
Patient: prediction horizon (h)	Number of seizures	No. of critical groups (g_{opt})	No. of electrodes in each group (k_{opt})	Sensitivity (%)	False prediction rate (false per hour)	Average warning time (min)
C: 3 h	15	2	3	85.71 (12/14)	0.111 (6/54.12)	75.9±14.0
C: 2 h	15	4	3	85.71 (12/14)	0.222 (12/54.12)	61.5±9.9
B: 3 h	10	4	3	100.00 (9/9)	0.131 (7/53.42)	106.1±15.6
B: 2 h	10	5	3	88.89 (8/9)	0.243 (13/53.42)	54.4±7.9
All patients: 3 h	25			91.30 (21/23)	0.121 (13/107.54)	88.8±14.7

Finally, the prediction algorithm was evaluated in a training and a testing mode. Half of the available datasets were used for training of the algorithm. The optimal parameters g and k were estimated based on the S and FPR performance of the algorithm on these training datasets (see Table 7). Then, the prediction algorithm ran on the remaining datasets (testing stage). The S, FPR and AWT of the algorithm were then estimated (see Table 8). We notice that the prospective seizure prediction algorithm predicted 5 out of the 7 seizures (71%) with a 0.15 FPR and about 80 min AWT for patient C, and 4 out of 4 seizures (100%) with a 0.14 FPR and about 75 min AWT for patient B. Overall, across patients, sensitivity of the algorithm was 81.82% with a false prediction rate of 1 false positive warning every 6.67 h.

4. Discussion

The results of this study support the feasibility of developing algorithms to predict impending seizures based on automated analysis of the spatiotemporal dynamical characteristics of multi-channel intracranial EEG recordings. The underlying principle is the existence of dynamical entrainment among critical sites of the epileptic brain prior to seizures. This study suggests that it may be possible to predict focal-onset epileptic seizures by analysis of measures of dynamics of multi-channel EEG signals, namely the rate of information production, or chaos, of a state in the corresponding state space.

Previous studies by our group have shown that there is a preictal transition, in which the values of the maximum Lyapunov exponents of EEG recorded from critical electrode sites converge long prior to a seizure's onset (Iasemidis et al., 2001). The electrode sites involved in this dynamical spatiotemporal interaction vary from seizure to seizure even in the same patient. Thus, the ability to predict a given seizure depends upon the ability to identify the critical electrode sites that participate in the preictal transition (Carney et al., 2001; Iasemidis et al., 1998; Sackellares et al., 2001). By employing a quadratic zero–one optimization technique for the selection of critical brain sites from the estimated STLmax profiles around a seizure, we demonstrated that the next seizure can be predicted 91.3% of the time, about 91 min prior to its onset, with the issue of 1 false warning every 8.27 h.

The prediction algorithm presented herein depends upon provided information about the exact time of occurrence of a seizure, because the update of the selected brain sites that are monitored thereafter for the prediction of the next seizure occurs at each seizure. Thus, this algorithm depends on a seizure detection algorithm that runs parallel to the prediction algorithm. We have developed an adaptive prediction algorithm that runs independently from a seizure

Table 7
Performance characteristics of SPA on the training datasets with parameters estimated from training datasets with the optimal parameters g and k per patient

Patient	Number of seizures	No. of critical groups (g_{opt})	No. of electrodes in each group (k_{opt})	Sensitivity (%)	False prediction rate (false warnings per hour)	Average warning time (min)
C: 2 h	8	4	5	71.43 (5/7)	0.18 (6/33.86)	41.7±44.4
B: 2 h	5	3	4	100.00 (4/4)	0.26 (5/19.38)	49.9±29.8
All patients	13			81.82 (9/11)	0.21 (11/53.24)	45.3±38.8

Table 8
Prospective prediction—testing of the SPA algorithm on the testing datasets

Patient	Number of seizures	Sensitivity (%)	False prediction rate (false per hour)	Average warning time (min)
C: 2 h	8	71.43 (5/7)	0.15 (3/20.26)	80.7±6.0
B: 2 h	5	100.00 (4/4)	0.14 (3/20.81)	74.9±15.3
All patients	13	81.82 (9/11)	0.15 (6/41.07)	78.1±11.0

Performance characteristics of SPA per patient with parameters estimated from the training datasets (see Table 7).

detection algorithm. In this algorithm, update of the sites to be monitored forward in time is performed irrespectively of the time of occurrence of the previous seizure. In this more advanced prediction scheme, a seizure detection algorithm is no longer necessary. These results are reported elsewhere (Iasemidis et al., 2003c). Evaluation of the prediction algorithm by dividing the available data into training and testing data sets is also reported therein. Optimal estimation of the prediction algorithm parameters g and k is then performed from the training data set, and subsequently applied to the testing data set. These prediction results are comparable with, and in many cases better than, the ones reported herein. More recent publications of our group point to the same direction (Carney et al., 2004; Chaovalitwongse et al., 2004a,b; Iasemidis et al., 2002b; Pardalos et al., 2003a,b; Sabesan et al., 2003a,b; Sackellares et al., 2004; Shiau et al., 2004; Veeramani et al., 2003a,b; Venugopal et al., 2003a,b).

We believe that the proposed techniques may become valuable for on-line, real-time seizure prediction. Such techniques could be incorporated into diagnostic and therapeutic devices for long-term monitoring and treatment of epilepsy. Potential diagnostic applications include a seizure warning system to be used during long-term EEG recordings, e.g. in a diagnostic epilepsy-monitoring unit. This type of system could be used to warn of an impending seizure for the patient or professional staff to take precaution measures or to trigger certain actions such as functional imaging procedures designed to measure regional cerebral blood flow during a seizure. Such a seizure warning algorithm, being implemented in digital signal processing chips, could also be incorporated into implantable therapeutic devices to timely activate implantable deep brain stimulators (DBS) or implantable drug-release reservoirs. These types of devices, if effective, could revolutionize the treatment of certain forms of epilepsy.

Acknowledgements

This research is supported by the National Institute of Biomedical Imaging and Bioengineering (NIBIB) via a Bioengineering Research Partnership grant for Brain Dynamics (8R01EB002089-03), NSF, DARPA and Whitaker Foundation. This material is the result of work supported with resources and the use of facilities at the Malcolm Randall VA Medical Center, Gainesville, Florida, and the Arizona State University, Tempe, Arizona.

References

Abarbanel HDI. Analysis of observed chaotic data. New York: Springer-Verlag; 1996.

Abou-Khalil BW, Siegel GJ, Sackellares JC, Gilman S, Hichwa R, Marshall R. Positron emission tomography studies of cerebral glucose metabolism in patients with chronic partial epilepsy. Ann Neurol 1987; 22:480–6.

Babb TL, Brown WJ. Pathological findings in epilepsy. In: Engel Jr. J, editor. Surgical Treatment of the Epilepsies. New York: Raven Press; 1987.

Babloyantz A, Destexhe A. Low dimensional chaos in an instance of epilepsy. Proc Natl Acad Sci USA 1986;83:3513–7.

Burdette DE, Sakuraisy, Henry TR, Ross DA, Pennell PB, Frey KA, Sackellares JC, Albin R. Temporal lobe central benzodiazepine binding in unilateral mesial temporal lobe epilepsy. Neurology 1995;45: 934–41.

Carney PR, Iasemidis LD, Pardalos PM, Srivastava A, Lee N, Won J, Shiau DS, MacLennan AJ, Sackellares JC. Predictability of seizures in an epilepsy-prone transgenic mouse model. Epilepsia 2001;S7:225 abstract.

Carney PR, Shiau D-S, Pardalos PM, Iasemidis LD, Chaovalitwongse W, Sackellares JC. Nonlinear neurodynamical features in an animal model of generalized epilepsy. In: Pardalos PM, Sackellares JC, Carney PR, Iasemidis LD, editors. Quantitative Neuroscience. Dordrecht: Kluwer Academic Publishers; 2004. p. 37–52.

Casdagli MC, Iasemidis LD, Sackellares JC, Roper SN, Gilmore RL, Savit RS. Characterizing nonlinearity in invasive EEG recordings from temporal lobe epilepsy. Physica D 1996;99:381–99.

Chaovalitwongse W, Pardalos PM, Iasemidis LD, Shiau D-S, Sackellares JC. Application of global optimization and dynamical systems to prediction of epileptic seizures. In: Pardalos PM, Sackellares JC, Carney PR, Iasemidis LD, editors. Quantitative Neuroscience. Dordrecht: Kluwer Academic Publishers; 2004a. p. 1–36.

Chaovalitwongse W, Pardalos PM, Iasemidis LD, Shiau D-S, Sackellares JC. Dynamical approaches and multi-quadratic integer programming for seizure prediction. J Optimization Methods Software; 2004b (in press).

De Lanerrole NC, Kim JH, Robbins RJ, Spencer DD. Hippocampal interneuron loss and plasticity in human temporal lobe epilepsy. Brain Res 1989;495:387–95.

Elger CE, Lehnertz K. Seizure prediction by non-linear time series analysis of brain electrical activity. Eur J Neurosci 1998;10:786–9.

Iasemidis LD. Epileptic seizure prediction and control. IEEE Trans Biomed Eng: Spec Issue Seizure Prediction 2003;50:549–58.

Iasemidis LD, Sackellares JC. The temporal evolution of the largest Lyapunov exponent on the human epileptic cortex. In: Duck DW, Pritchard WS, editors. Measuring Chaos in the Human Brain. Singapore: World Scientific; 1991. p. 49–82.

Iasemidis LD, Sackellares JC. Chaos theory and epilepsy. Neuroscientist 1996;2:118–26.

Iasemidis LD, Sackellares JC, Zaveri HP, Williams WJ. Phase space topography of the electrocorticogram and the Lyapunov exponent in partial seizures. Brain Topogr 1990;2:187–201.

Iasemidis LD, Sackellares JC, Savit RS. Quantification of hidden time dependencies in the EEG within the framework of nonlinear dynamics. In: Jansen BH, Brandt ME, editors. Nonlinear dynamical analysis of the EEG. Singapore: World Scientific; 1993. p. 30–47.

Iasemidis LD, Olson LD, Sackellares JC, Savit RS. Time dependencies in the occurrences of epileptic seizures: a nonlinear approach. Epilepsy Res 1994;17:81–94.

Iasemidis LD, Principe JC, Sackellares JC. Spatiotemporal dynamics of human epileptic seizures. In: Harrison RG, Weiping L, Ditto W, Pecora L, Vohra S, editors. Third Experimental Chaos Conference. Singapore: World Scientific; 1996. p. 26–30.

Iasemidis LD, Principe JC, Czaplewski JM, Gilman RL, Roper SN, Sackellares JC. Spatiotemporal transition to epileptic seizures: a nonlinear dynamical analysis of scalp and intracranial EEG recordings. In: Lopes da Silva F, Principe JC, Almeida LB, editors. Spatiotemporal Models in Biological and Artificial Systems. Amsterdam: IOS Press; 1997. p. 81–8.

Iasemidis LD, Sackellares JC, Gilmore RL, Roper SN. Automated seizure prediction paradigm. Epilepsia 1998;39(S6):207 abstract.

Iasemidis LD, Shiau D-S, Pardalos PM, Sackellares JC. Transition to epileptic seizures—an optimization approach into its dynamics. In: Du DZ, Pardalos PM, Wang J, editors. Discrete problems with medical applications. DIMACS series 55. Providence, RI: American Mathematical Society Publishing Co.; 2000a. p. 55–74.

Iasemidis LD, Principe JC, Sackellares JC. Measurement and quantification of spatiotemporal dynamics of human epileptic seizures. In: Akay M, editor. Nonlinear biomedical signal processing, vol. II. IEEE Press; 2000b. p. 294–318.

Iasemidis LD, Pardalos PM, Sackellares JC, Shiau D-S. Quadratic binary programming and dynamical system approach to determine the predictability of epileptic seizures. J Comb Optimization 2001;5:9–26.

Iasemidis LD, Shiau D-S, Pardalos PM, Sackellares JC. Phase entrainment and predictability of epileptic seizures. In: Pardalos PM, Principe JC, editors. Biocomputing. Dordrecht: Kluwer Academic Publishers; 2002. p. 59–84.

Iasemidis LD, Pardalos PM, Yatsenko VA, Sackellares JC. Global optimization approaches to reconstruction of dynamical systems related to epileptic seizures. In: Fotiadis D, Massalas CV, editors. Scattering and Biomedical Engineering: Modeling and Applications.. Singapore: World Scientific; 2002. p. 308–18.

Iasemidis LD, Pardalos PM, Shiau D-S, Chaovalitwongse W, Narayanan K, Kumar S, Carney PR, Sackellares JC. Prediction of human epileptic seizures based on optimization and phase changes of brain electrical activity. J Optimization Methods Software 2003a;18:81–104.

Iasemidis LD, Prasad A, Sackellares JC, Pardalos PM, Shiau D-S. On the prediction of seizures, hysteresis and resetting of the epileptic brain: insights from models of coupled chaotic oscillators. In: Bountis T, Pneumatikos S, editors. Order and Chaos. Thessaloniki, Greece: Publishing House of K. Sfakianakis; 2003b. p. 283–305.

Iasemidis LD, Shiau D-S, Chaovalitwongse W, Sackellares JC, Pardalos PM, Principe JC, Carney PR, Prasad A, Veeramani B, Tsakalis K. Adaptive epileptic seizure prediction system. IEEE Trans Biomed Eng, Spec Issue Seizure Prediction 2003c;50:616–27.

Iasemidis LD, Shiau D-S, Sackellares JC, Pardalos PM, Prasad A. Dynamical resetting of the human brain at epileptic seizures: application of nonlinear dynamics and global optimization techniques. IEEE Trans Biomed Eng 2004a;51(3):493–506.

Iasemidis LD, Tsakalis K, Sackellares JC, Pardalos PM. Comments on the Inability of Lyapunov exponents to predict epileptic seizures. Phys Rev Lett; 2004b (in press).

Jansen BH. Is it and so what? A critical review of EEG-chaos. In: Duke DW, Pritchard WS, editors. Measuring Chaos in the Human Brain. Singapore: World Scientific; 1991. p. 49–82.

Kostelich EJ. Problems in estimating dynamics from data. Physica D 1992; 58:138–52.

Lai YC, Harrison MAF, Frei MG, Osorio I. Inability of Lyapunov exponents to predict epileptic seizures. Phys Rev Lett 2003;91: 0681021–0681024.

Lai YC, Harrison MAF, Frei MG, Osorio I. Controlled test for predictive power of Lyapunov exponents: their inability to predict epileptic seizures. Chaos 2004;(14):630–42.

Le Van Quyen M, Martinerie J, Baulac M, Varela F. Anticipating epileptic seizures in real time by non-linear analysis of similarity between EEG recordings. NeuroReport 1999;10:2149–55.

Le Van Quyen M, Martinerie J, Navarro V, Boon P, D'Havé M, Adam C, Renault B, Varela F, Baulac M. Anticipation of epileptic seizures from standard EEG recordings. Lancet 2001;357:183–8.

Lehnertz K, Elger CE. Can epileptic seizures be predicted? Evidence from nonlinear time series analysis of brain electrical activity Phys Rev Lett 1998;80:5019–22.

Lehnertz K, Litt B. The first international collaborative workshop on seizure prediction: summary and data descriptions (2004), This issue.

Martinerie J, Adam C, Le Van Quyen M, Baulac M, Clemenceu S, Renault B, Varela FJ. Epileptic seizures can be anticipated by non-linear analysis. Nat Med 1998;4:1173–6.

McDonald JW, Garofalo EA, Hood T, Sackellares JC, Gilman S, McKeever PE, Troncaso JC, Johnston MV. Altered excitatory and inhibitory amino acid receptor binding in hippocampus of patients with temporal lobe epilepsy. Ann Neurol 1991;29:529–41.

Niedermeyer E. Depth electroencephalography. In: Niedermeyer E, Lopes da Silva F, editors. Electroencephalography: Basic Principles, Clinical Applications and Related Fields. Baltimore: Urban and Schwarzenberg; 1987. p. 593–617.

Oseledec A. A multiplicative ergodic theorum—Lyapunov characteristic numbers for dynamical systems (English translation). IEEE Int Conf ASSP 1968;19:179–210.

Packard NH, Crutchfield JP, Farmer JD, Shaw RS. Geometry from time series. Phys Rev Lett 1980;45:712–6.

Pardalos PM, Rodgers G. Parallel branch and bound algorithms for unconstrained quadratic zero–one programming. In: Sharda R, et al., editor. Impact of Recent Computer Advances on Operations Research. North-Holland; 1989.

Pardalos PM, Rodgers G. Computational aspects of a branch and bound algorithm for quadratic zero–one programming. Computing 1990;45: 131–44.

Pardalos PM, Sackellares JC, Iasemidis LD, Yatsenko V, Yang MCK, Shiau D-S, Chaovalitwongse W. Statistical information approaches to modeling and detection in the human brain. Comput Stat Data Anal 2003a;43:79–108.

Pardalos PM, Yatsenko VA, Sackellares JC, Shiau DS, Chaowolitwongse W, Iasemidis LD. Analysis of EEG data using optimization statistics, and dynamical system techniques. Comput Stat Data Anal 2003b;44(1–2):391–408.

Pennell PB, Burdette DE, Ross DA, Henry TR, Albin RL, Sackellares JC, Frey KA. Muscarinic receptor loss and preservation of presynaptic cholinergic terminals in hippocampal sclerosis. Epilepsia 1999;40: 38–46.

Pesin J. Characteristic Lyapunov exponents and smooth ergodic theory. Russ Math Surv 1977;4:55–114.

Sabesan S, Narayanan K, Prasad A, Spanias A, Iasemidis LD. Improved measure of information flow in coupled nonlinear systems. Proc IASTED (Int Assoc Sci Technol Dev) Int Conf 2003a:329–33.

Sabesan S, Narayanan K, Prasad A, Spanias A, Sackellares JC, Iasemidis LD. Predictability of Epileptic Seizures: A Comparative Study Using Lyapunov Exponent and Entropy Based Measures. Proceedings of the 40th Annual Rocky Mountain Bioengineering Symposium.: ISA Publishing; 2003b; pp. 129–135.

Sackellares JC, Iasemidis LD, Gilmore RL, Roper SN. Epileptic seizures as neural resetting mechanisms. Epilepsia 1997;S3:189 abstract.

Sackellares JC, Iasemidis LD, Shiau D-S. Detection of preictal transition in scalp EEG. Epilepsia 1999;40:176 abstract.

Sackellares JC, Iasemidis LD, Shiau D-S, Gilmore RL, Roper SN. Epilepsy—when chaos fails. In: Lehnertz K, Arnhold J, Grassberger P, Elger CE, editors. Chaos in the Brain?. Singapore: World Scientific; 2000. p. 112–33.

Sackellares JC, Iasemidis LD, Pardalos PM, Chaovalitwongse W, Shiau DS, Roper SN, Gilmore RL, Carney PR, Principe JC. Performance characteristics of an automated seizure warning algorithm utilizing dynamical measures of the EEG signal and global optimization techniques. Epilepsia 2001;42(S7):40 abstract.

Sackellares JC, Iasemidis LD, Pardalos PM, Shiau D-S. Combined application of global optimization and nonlinear dynamics to detect state resetting in human epilepsy. In: Pardalos PM, Principe JC, editors. Biocomputing. Dordrecht: Kluwer Academic Publishers; 2002. p. 140–58.

Sackellares JC, Iasemidis LD, Shiau DS, Pardalos PM, Carney PR. Spatiotemporal transitions in temporal lobe epilepsy. In: Pardalos PM, Sackellares JC, Carney PR, Iasemidis LD, editors. Quantitative Neuroscience. Dordrecht: Kluwer Academic Publishers; 2004. p. 223–38.

Savic I, Roland P, Sedvall G, Persson A, Pauli S, Widen L. In-vivo demonstration of reduced benzodiazepine receptor-binding in human epileptic foci. Lancet 1988;2:863–6.

Shiau DS, Luo Q, Gilmore RL, Roper SN, Pardalos PM, Sackellares JC, Iasemidis LD. Epileptic seizures resetting revisited. Epilepsia 2000;S7: 208–9 abstract.

Shiau DS, Chaovalitwongse W, Iasemidis LD, Pardalos PM, Carney PR, Sackellares JC. Nonlinear dynamical and statistical approaches to investigate dynamical transitions before epileptic seizures. In: Pardalos PM, Sackellares JC, Carney PR, Iasemidis LD, editors. Quantitative Neuroscience. Dordrecht: Kluwer Academic Publishers; 2004. p. 239–50.

Spencer SS, Jung K, Spencer DD. Ictal spikes: a marker of specific hippocampal cell loss. Electroenceph Clin Neurophysiol 1992;83: 104–11.

Takens F. Detecting strange attractors in turbulence. In: Rand DA, Young LS, editors. Dynamical Systems and Turbulence, Lecture Notes in Mathematics. Heidelburg: Springer-Verlag; 1981.

Vastano JA, Kostelich EJ. Comparison of algorithms for determining Lyapunov exponents from experimental data. In: Mayer-Kress G, editor. Dimensions and entropies in chaotic systems: quantification of complex behavior. New York: Springer-Verlag; 1986. p. 100–7.

Veeramani B, Narayanan K, Prasad A, Spanias A, Iasemidis LD. On the use of the directed transfer function for nonlinear systems. Proc IASTED Int Conf 2003a;270–4.

Veeramani B, Prasad A, Narayanan K, Spanias A, Iasemidis LD. Measuring Information Flow in Nonlinear Systems—A Modeling Approach in the State Space. Proceedings of the 40th Annual Rocky Mountain Bioengineering Symposium.: ISA Publishing; 2003b pp. 65–70.

Venugopal R, Narayanan K, Prasad A, Spanias A, Sackellares JC, Iasemidis LD. A new approach towards predictability of epileptic seizures: KLT dimension. Proceedings of the 40th Annual Rocky Mountain Bioengineering Symposium.: ISA Publishing; 2003a pp. 123–128.

Venugopal R, Prasad A, Narayanan K, Spanias A, Iasemidis LD. Nonlinear noise reduction and predictability of epileptic seizures. Proc IASTED Int Conf 2003b;240–5.

Walters P. An Intorduction to Ergodic Theory. Berlin: Springer-Verlag; 1982.

Witte H, Iasemidis LD, Litt B. Towards epileptic seizure prediction and control: a survey of methods and models. IEEE Trans Biomed Eng, Spec Issue Seizure Prediction, Ed 2003;50:537–9.

Wolf A, Swift JB, Swinney HL, Vastano JA. Determining Lyapunov exponents from a time series. Physica D 1985;16:285–317.